24th COBEM - 2017

24th ABCM International Congress of Mechanical Engineering
December 3-8, 2017, Curitiba, PR, Brazil

COBEM-2017-2346
TRANSPORT THROUGH POLYMER LAYER AND POROUS ARTERIAL WALL WITH BINDING IN DRUG-ELUTING STENTS USING THE FEM

Rachel Lucena
Norberto Mangiavacchi
José Pontes
Gustavo Anjos
State University of Rio de Janeiro, Rio de Janeiro, RJ, Brazil
rachel.lucena@gmail.com,norberto.mangiavacchi@gmail.com, jose.pontes@uerj.br, gustavo.anjos@uerj.br

Sean McGinty
Division of Biomedical Engineering, University of Glasgow, Glasgow, UK
sean.mcginty@glasgow.ac.uk

Abstract. *The safety and efficacy of Drug-eluting stents is strongly influenced by the transport of the antiproliferative/anti-inflammatory drugs in the arterial wall. Dissolution in the polymer coating and specific binding in the artery wall play an important role in the process. We consider the model of dissolution, transport and binding of sirolimus on an axisymmetric domain representing the polymer coating layer and the porous artery wall in the vicinity of a stent strut. We employ the FEM on an unstructured mesh to discretise the governing equations. We employ a nonlinear dissolution model for the dynamics in the coating, and a nonlinear saturable binding model that includes both specific and non-specific binding in the arterial wall as separate phases, as proposed by McGinty and Pontrelli (2016). The arterial wall is considered an anisotropic porous media, and the flow is considered to be governed by Darcy flow. The permeability in the polymer coating is considered to be very small, but finite. The endothelium lamina, where present, is modelled as a no-flow boundary. The effect of slow and fast release polymers is considered, showing that the time evolution of the process can be efficiently controlled by the polymer diffusion coefficient. However, the spatial distribution of the sirolimus is greatly influenced by the flow and the arterial wall properties, being therefore susceptible to patient health conditions.*

Keywords: *drug-eluting stents, Darcy's law, convection-diffusion-reaction equations, finite element method*

1. INTRODUCTION

Drug-eluting stents (DES) marked a technology breakthrough in the field of percutaneous coronary intervention (PCI) due to a profound reduction in neointimal hyperplasia and the need for repeat revascularization as compared with bare-metal stents (BMS). However several concerns related to a higher risk of late thrombotic events and catch-up in efficacy during long-term follow-up hampered their widespread adoption in clinical practice, according to Chisari *et al.* (2016).

In DES, safety and efficacy are strongly influenced by the transport of the antiproliferative/anti-inflammatory drugs in the arterial wall. Dissolution in the polymer coating and specific binding in the artery wall play an important role in the process.

We consider the model of dissolution, transport and binding of sirolimus on an axisymmetric domain representing the polymer coating layer and the porous artery wall in the vicinity of a stent strut. We employ the FEM on an unstructured mesh to discretise the governing equations. We employ a nonlinear dissolution model for the dynamics of sirolimus in the polymer coating, and a nonlinear saturable binding model that includes both specific and non-specific binding in the arterial wall as separate phases, as proposed by McGinty and Pontrelli (2016). The arterial wall is considered an anisotropic porous media, and the flow is considered to be governed by Darcy flow. The effect of slow and fast release polymers is considered, showing that the time evolution of the process can be efficiently controlled by the polymer diffusion coefficient. However, the spatial distribution of the sirolimus is greatly influenced by the flow and the arterial wall properties, being therefore susceptible to patient health conditions.

2. THE MATHEMATICAL MODEL

In this work we assume a geometric symmetry about a reference axis, and therefore we employ an axisymmetric formulation. Figure 1 shows the model geometry where z direction is the axis of symmetry and r is the radial direction.

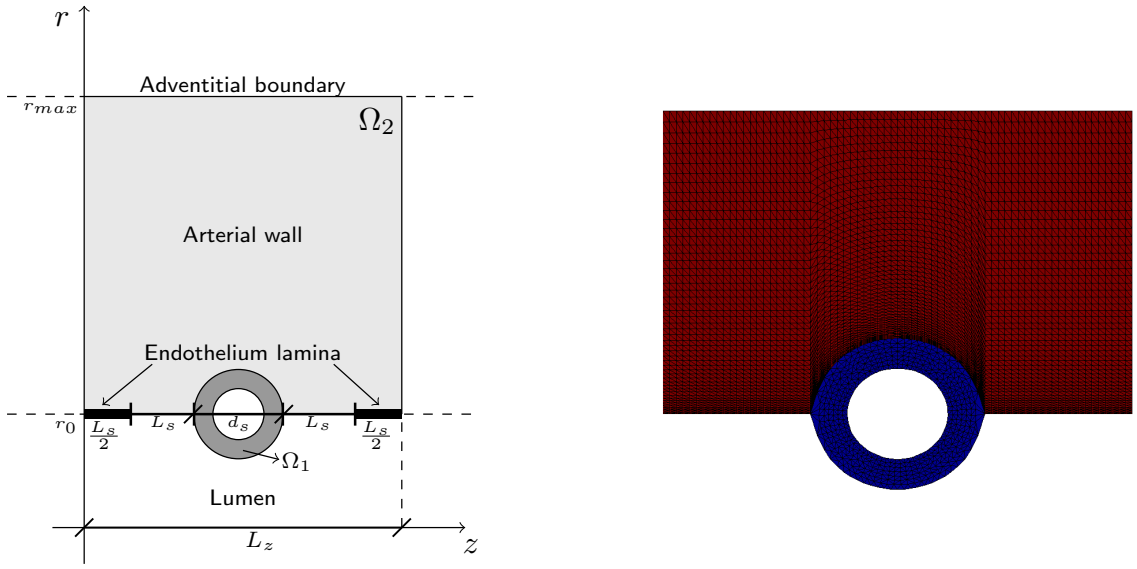

Figure 1. Left: Model 2D axisymmetric geometry. Note that the endothelium is assumed to be denuded in the vicinity of the stent strut. Right: Computational domain and unstructured triangular mesh employed in the simulations. Blue: polymer layer Ω_1. Red: arterial wall Ω_2.

The region Ω_1 represents the polymer layer and Ω_2 represents the arterial wall.

We adopt the modelling framework of McGinty and Pontrelli (2016) and Bozsak *et al.* (2014). The drug dynamics in the coating is modelled in terms of b_0 (solid) and c_0 (dissolved) concentrations by the equations:

$$\frac{\partial b_0}{\partial t} = -\beta_0 b_0^{2/3}(S_0 - c_0) \tag{1}$$

$$\frac{\partial c_0}{\partial t} = \nabla \cdot (\mathcal{D}_0 \nabla c_0) + \beta_0 b_0^{2/3}(S_0 - c_0), \tag{2}$$

where $\mathcal{D}_0$ is the effective scalar diffusion coefficient of the solute, β_0 the dissolution rate and S_0 is the solubility limit.

The arterial wall and the polymer layer are considered as porous media, and flow within these layers is assumed to be governed by Darcy's law, thus

$$\mathbf{u} = -\kappa_i \nabla p, \tag{3}$$

where $\mathbf{u} = (u, v)$ is the velocity field, p is the pressure in the arterial wall, $\kappa_i = P_{Di}/\mu$, P_{Di} is the Darcy permeability of the media and μ is the fluid viscosity. Assuming the continuity equation $\nabla \cdot \mathbf{u} = 0$, we can rewrite the Eq. 3:

$$\nabla \cdot (-\kappa_i \nabla p) = 0. \tag{4}$$

Drug elution in the arterial wall is governed by the convection-diffusion-reaction equation:

$$\frac{Dc_1}{Dt} = \nabla \cdot (\mathcal{D}_1 \nabla c_1) - k_1^f c_1 (b_1^{max} - b_1) + k_1^r b_1 - k_2^f c_1 (b_2^{max} - b_2) + k_2^r b_2 \tag{5}$$

$$\frac{\partial b_1}{\partial t} = k_1^f c_1 (b_1^{max} - b_1) - k_1^r b_1 \tag{6}$$

$$\frac{\partial b_2}{\partial t} = k_2^f c_1 (b_2^{max} - b_2) - k_2^r b_2 \tag{7}$$

where c_1 is the concentration of a drug transported in the arterial wall, the operator D/Dt is the material derivative, b_1 and b_2 denote non-specifically and specifically bound drug, respectively, k_i^f, k_i^r, b_i^{max} are constant parameters related to the binding kinetics, $\mathcal{D}_1$ is diffusion coefficient, given by the tensor:

$$\mathcal{D}_1 = \begin{bmatrix} \mathcal{D}_{1r} & 0 \\ 0 & \mathcal{D}_{1z} \end{bmatrix},$$

with r the radial direction and z the axial direction.

The permeability in the polymer coating, P_{D0}, is considered to be very small, but finite. The endothelium lamina, where present, is modelled as a no-flow boundary. The boundary conditions on drug in the denuded endothelium is $c_1 = 0$, and between polymer and blood, i.e., on interface Γ_1 is $c_0 = 0$ (see Fig. 2), and in the interior surface of Ω_1 we impose zero flux (see Fig. 1, left). We assume periodic conditions at the side boundaries.

The mass flux is established across the interface and the drug starts to be transferred to the adjacent release medium. The instantaneous flux is given by:

$$\phi_i(t) = \int_{\Gamma_i} \mathbf{n} \cdot \mathcal{D}_0 \nabla c_0(t) d\Gamma, \quad \text{with} \quad i = 1, 2, \tag{8}$$

where $i = 1$ refers to the lumen interface, and $i = 2$ refers to the arterial wall (see Fig. 2). $d\Gamma = 2\pi r ds$ and the mass flux (integral) is given by:

$$\Phi_i = \int_0^t \phi_i(t) dt, \tag{9}$$

where t is the time.

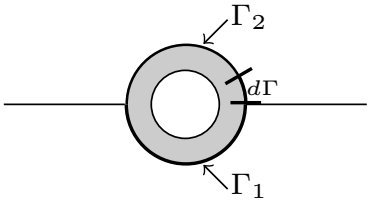

Figure 2. Sketch of interface polymer-lumen and polymer-arterial wall.

The volume averaged total solid and bound sirolimus concentration is defined as:

$$\bar{B}(t) = \frac{1}{V} \int_V (b_0 + b_1 + b_2)(t) dV, \tag{10}$$

where V is the volume of the polymer. Similarly, the volume averaged total free sirolimus concentration is:

$$\bar{C}(t) = \frac{1}{V} \int_V (c_0 + c_1)(t) dV, \tag{11}$$

in both Eqs.(10) and (11) the unit is mol·m^{-3}.

When the flux tends asymptotically at lumen and artery wall boundaries, it is possible to measure the relationship between them, so we have:

$$R_1 = \frac{\Phi_1(t \to \infty)}{\Phi_1(t \to \infty) + \Phi_2(t \to \infty)} \tag{12}$$

and

$$R_2 = \frac{\Phi_2(t \to \infty)}{\Phi_1(t \to \infty) + \Phi_2(t \to \infty)}, \tag{13}$$

where R_1 and R_2 denote the relationship between integral flux in the boundary Γ_1 and Γ_2.

3. NUMERICAL METHOD

The governing equations in 2D axisymmetric coordinates are solved on an unstructured triangular mesh, using linear base functions and the Galerkin Finite Element Method (see Lucena, 2016). The convective terms are discretised using a semi-Lagrangian approach. The Darcy flow is considered to be steady, and driven by the average pressure difference between the lumen and the adventitial boundary (outer boundary of the arterial wall). A semi-implicit fractional step method is employed for the convection-diffusion-reaction equations. The dimensional parameters employed in the simulations are shown in Tab. 1.

Table 1. Dimensional parameters used in the simulations

Parameter		Simulated value	Reference
r_0	lumen radius	1.5×10^{-3}m	Bozsak *et al.* (2014)
$r_{max} - r_0$	arterial wall thickness	5.0×10^{-4}m	Bozsak *et al.* (2014)
d_s	stent strut diameter	2.5×10^{-4}m	Bozsak *et al.* (2014)
L_s	denuded endothelium	1.5×10^{-4}m	Bozsak *et al.* (2014)
L_p	polymer thickness	5.0×10^{-5}m	Bozsak *et al.* (2014)
L_z	domain length	7.0×10^{-4}m	Bozsak *et al.* (2014)
p_{wall}	lumen overpressure	9.31×10^3 Pa	Bozsak *et al.* (2014)
μ	fluid viscosity	7.2×10^{-4} Pa s	Bozsak *et al.* (2014)
dt	simulation time step	100s	
t_{end}	time of simulation	20 and 200 days	
	Polymer layer		
P_{D0}	permeability	2.78×10^{-21}m^2	
β_0	dissolution rate	1.0×10^{-4}(mol m^{-3})$^{-2/3}$ s^{-1}	McGinty and Pontrelli (2016)
B_0	initial drug eluting	100 mol m^{-3}	McGinty and Pontrelli (2016)
S_0	drug solubility	$B_0/10$ mol m^{-3}	McGinty and Pontrelli (2016)
$\mathcal{D}_0$	fast diffusion coefficient	1.0×10^{-14}m^2 s^{-1}	Bozsak *et al.* (2014)
$\mathcal{D}_0$	slow diffusion coefficient	1.0×10^{-15}m^2 s^{-1}	
	Sirolimus		
P_{D1}	permeability	2.0×10^{-18}m^2	Bozsak *et al.* (2014)
$\mathcal{D}_{1r}$	radial diffusion coefficient	7×10^{-12}m^2 s^{-1}	Bozsak *et al.* (2014)
$\mathcal{D}_{1z}$	axial diffusion coefficient	4×10^{-11}m^2 s^{-1}	Bozsak *et al.* (2014)
k_1^f		2 (mol m^{-3} s)$^{-1}$	McGinty and Pontrelli (2016)
k_1^r		5.2×10^{-3} s^{-1}	McGinty and Pontrelli (2016)
b_1^{max}		3.63×10^{-1} mol m^{-3}	McGinty and Pontrelli (2016)
k_2^f		800 (mol m^{-3} s)$^{-1}$	McGinty and Pontrelli (2016)
k_2^r		$1.6 \times 10^{-4} s^{-1}$	McGinty and Pontrelli (2016)
b_2^{max}		3.3×10^{-3} mol m^{-3}	McGinty and Pontrelli (2016)

4. COMPUTATIONAL RESULTS AND DISCUSSION

The pressure and velocity distributions are shown in Figs. 3 and 4. These distributions are assumed constant along the simulation of the sirolimus transport.

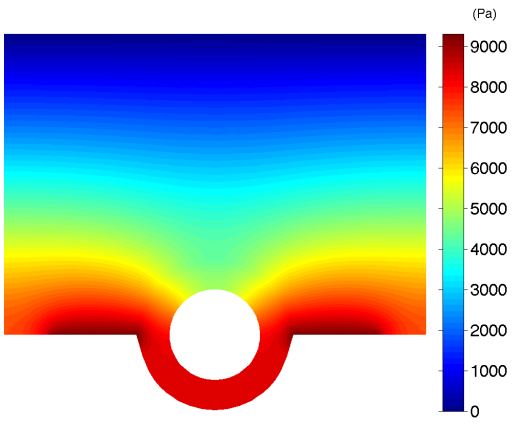

Figure 3. Pressure distribution obtained by the solution of Darcy Eq. (4).

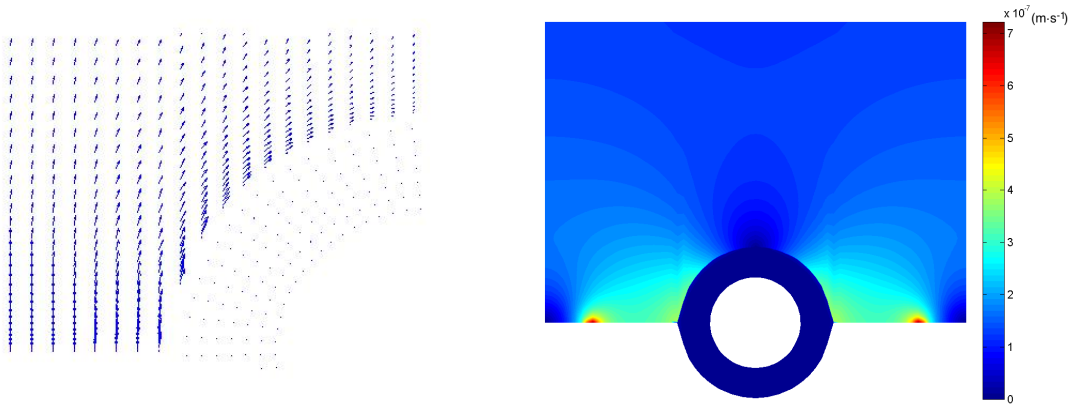

(a) (b)

Figure 4. (a) Velocity field showing relatively large flow velocity close to the junction of the denuded endothelium and the polymer layer, with $\mathbf{u}_{\max} = 7.229 \times 10^{-7}$ m·s^{-1}; (b) Magnitude of velocity computed from Eq. (3).

The simulation starts with all the sirolimus in solid form in the polymer layer, with concentration B_0, and null concentration elsewhere. The solid sirolimus gradually dissolves in the polymer layer and diffuses to the porous artery wall, where it is convected-diffused-bound (see Figs. 5 to 7, and Figs. 9 to 11).

However, even being quite stable during a long time interval, sirolimus concentration is very uneven along the artery wall, showing relatively large concentrations on the top of the struts, and low concentrations on the regions of denuded endothelium, due to the convection and the velocity patterns of the Darcy flow (Fig. 4). A sensitivity analysis is performed (not shown) demonstrating that changes in permeability and diffusivity in the arterial wall, that could be associated to patient conditions, greatly affect the spatial distribution of the sirolimus concentration.

4.1 Fast release polymer

Figures 5, 6, and 7 show the concentration of dissolved and bound sirolimus in the case of a fast release polymer.

Figure 5 shows that the sirolimus distribution at $t = 2$ days and $t = 20$ days is qualitatively similar, however at $t = 20$ days the concentration is 5 orders of magnitude smaller than at $t = 2$ days.

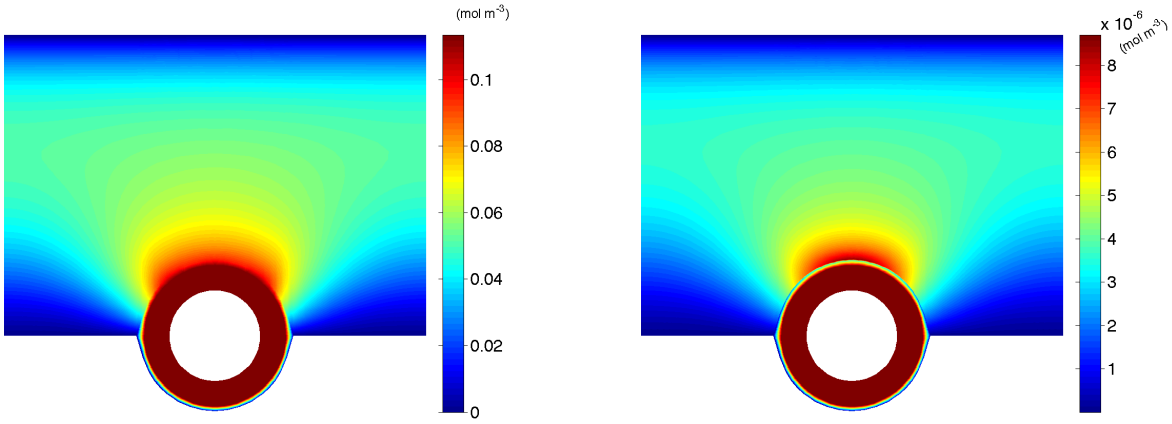

(a) $t = 2$ days (b) $t = 20$ days

Figure 5. Results of sirolimus concentration for fast release polymer at two stages of a simulation: 2 and 20 days, respectively. Concentration of free sirolimus at the artery wall and polymer layer.

Figure 6 shows that the solid (in the polymer) and specific bound (in the arterial wall) sirolimus distribution at $t = 2$ days and $t = 20$ days is dramatically different, since at $t = 2$ days there is a large quantity of solid (undissolved) sirolimus in the polymer, while at $t = 20$ days all the solid sirolimus has been dissolved, and the bound sirolimus in the arterial wall is gradually decaying. The decay of the specific bound sirolimus is a source for the dissolved sirolimus concentration, as seen in Eq. 5, and it is responsible for the distribution seen at later times in Fig. 5 (b).

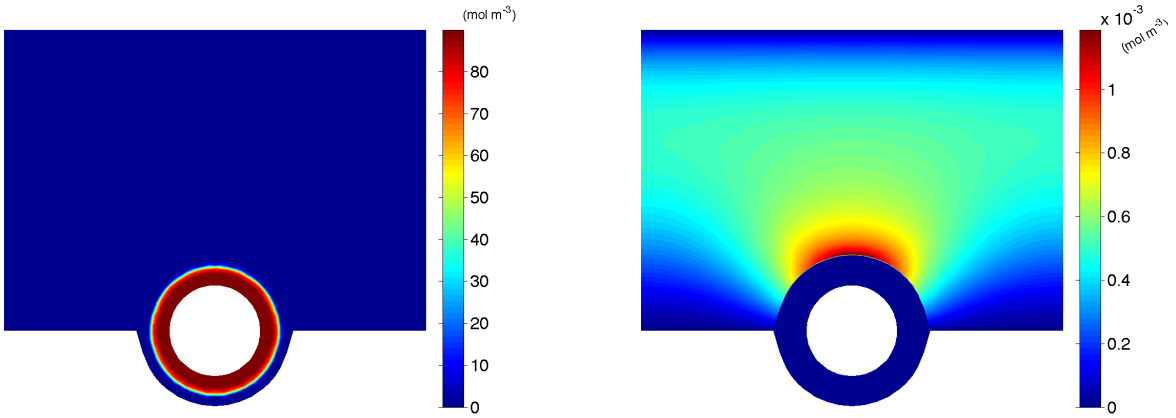

(a) $t = 2$ days (b) $t = 20$ days

Figure 6. Solid (b0) and non-specifically bound (b1) sirolimus for fast release polymer at two stages of a simulation: 2 and 20 days, respectively.

Figure 7 shows that the non-specifically bound (in the artery wall) sirolimus distribution at $t = 2$ days and $t = 20$ days is very uniform in the arterial wall, due to the low value of saturation. At time $t = 20$ days the non-specific bound (in the artery wall) sirolimus concentration is still quite uniform, due to the low kinetic coefficient value k_2^r.

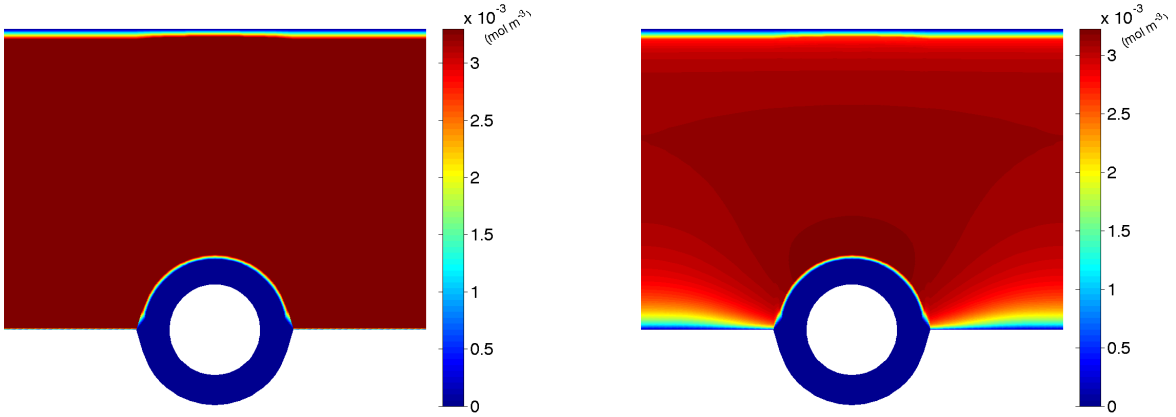

(a) $t = 2$ days (b) $t = 20$ days

Figure 7. Specifically bound (b2) sirolimus for fast release polymer at two stages of a simulation: 2 and 20 days, respectively.

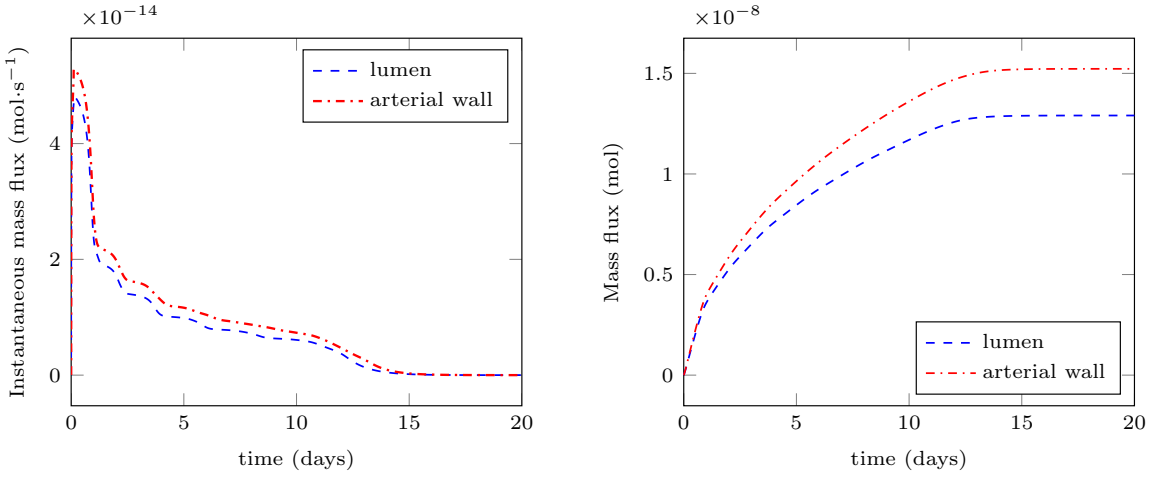

(a) (b)

Figure 8. (a) Sirolimus flux (instantaneous) ϕ_i, and (b) sirolimus flux (integral) Φ_i for fast release polymer.

4.2 Slow release polymer

Figures 9, 10, and 11 show the concentration of dissolved and bound sirolimus in the case of a slow release polymer. Results are qualitatively similar to the fast release polymer, however the time evolution is much slower.

Similarly to Fig. 5, Fig. 9 shows that the sirolimus distribution at $t = 20$ days and $t = 200$ days is qualitatively similar, however at $t = 200$ days the concentration is 4 orders of magnitude smaller than at $t = 20$ days.

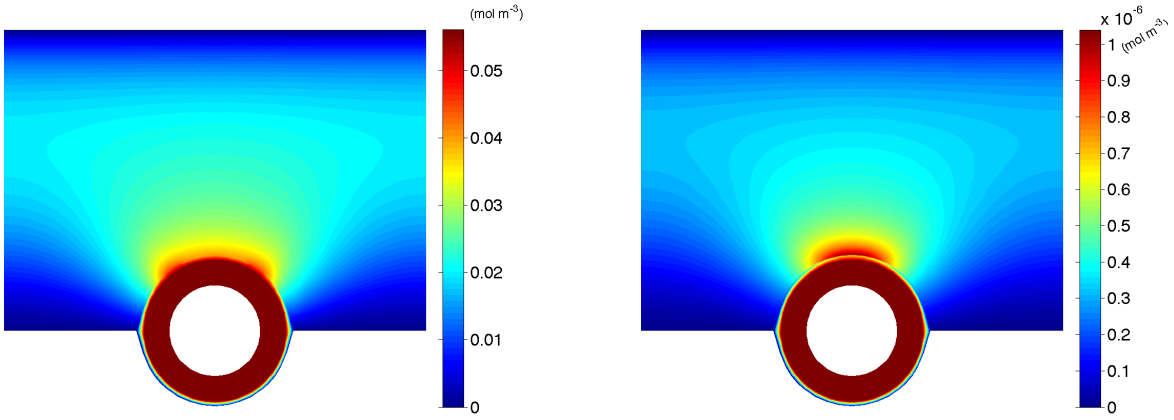

(a) $t = 20$ days (b) $t = 200$ days

Figure 9. Results of sirolimus concentration for slow release at two stages of a simulation: 20 and 200 days, respectively. Concentration of free sirolimus at the artery wall and polymer layer.

Figure 10 at time $t = 20$ days is similar to Fig. 6 at time $t = 2$ days. However the dissolution is more uneven in the case of the slow release.

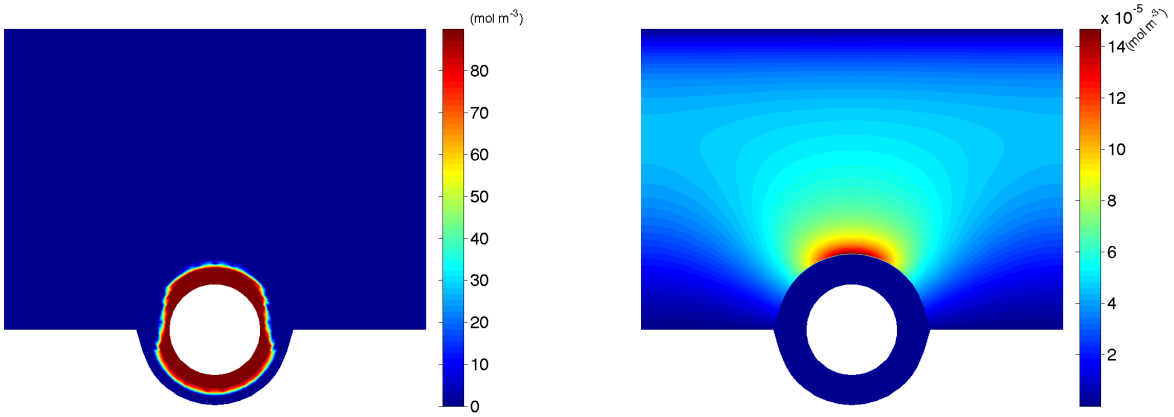

(a) $t = 20$ days (b) $t = 200$ days

Figure 10. Solid (b0) and non-specifically bound (b1) sirolimus for slow release polymer at two stages of a simulation: 20 and 200 days, respectively.

Figure 11 at time $t = 20$ days is similar to Fig. 7 at time $t = 2$ days. However, comparing the result for slow release at time $t = 200$ days (Fig. 11(b)) and the result for fast release at time $t = 20$ days (Fig. 7(b)), it is noticeable a stronger decay in (Fig. 11(b)), which is due to the much longer evolution time.

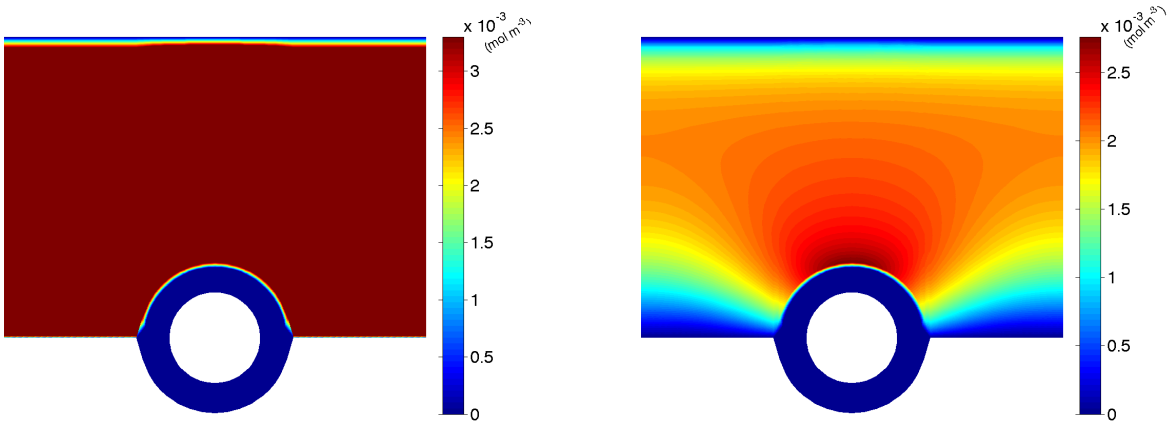

(a) $t = 20$ days (b) $t = 200$ days

Figure 11. Specifically bound b_2 sirolimus for slow release polymer at two stages of a simulation: 20 and 200 days, respectively.

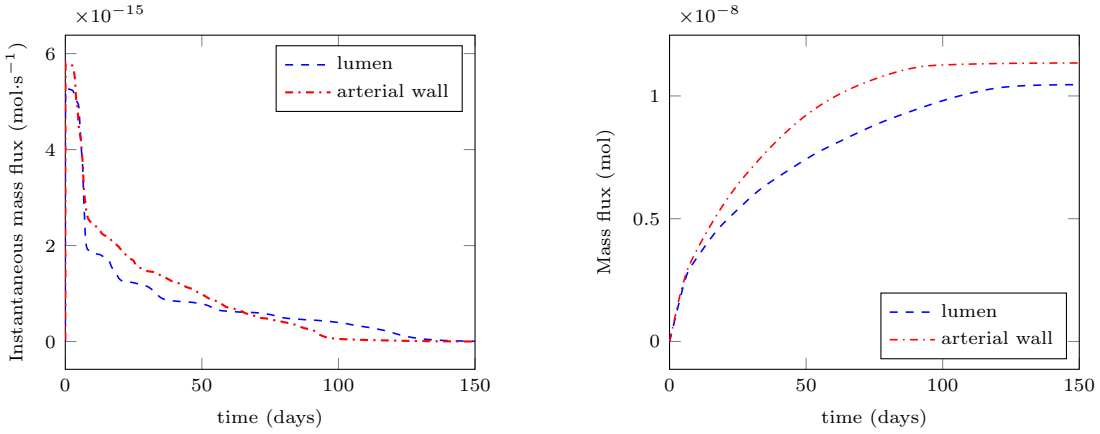

(a) (b)

Figure 12. (a) Sirolimus flux (instantaneous) ϕ_i, and (b) sirolimus flux (integral) Φ_i for slow release polymer.

4.3 Sirolimus concentration flux and volume averaged concentration

Figures 8 and 12 show the evolution of the instantaneous flux ϕ_i (Eq. 8) and integral flux Φ_i (Eq. 9) to the artery wall and to artery lumen. It can be seen that, for the fast release polymer, Fig. 8(a), the flux ϕ_2 to the wall is always larger than the flux ϕ_1 to the lumen. In the case of slow release polymer, Fig. 12(a), the flux ϕ_2 to the wall is larger than the flux ϕ_1 to the lumen most of the time, but ϕ_1 has a slower decay and eventually becomes larger than ϕ_2, reversing the initial trend.

The integral flux Φ_i computation shows that for fast release polymer coating, as can be seen in Fig. 8(b), about 46% of the sirolimus is transported to the arterial lumen ($R_1 \approx 0.46$), and 54% is transported to the arterial wall ($R_2 \approx 0.54$). Similarly for slow release polymer coating, Fig. 12(b), about 48% of the sirolimus is transported to the artery lumen ($R_1 \approx 0.48$), and 52% is transported to the arterial wall ($R_2 \approx 0.52$).

Simulations show that after a short initial time, while undissolved sirolimus concentration is higher than the saturation concentration in the polymer, the concentration in the artery wall varies very slowly in time (Fig. 13). Once the solid sirolimus is depleted, the concentration in the artery wall falls sharply. This happens soon after day 12 and the sirolimus concentration drops to almost zero by day 15 in the in the case of fast release polymer, and by day 120 in the case of slow release polymer. At this stage the binding process reverses and the bound sirolimus decay feeds the drug back to the c_1 unbound concentration. While for the fast release polymer the solid and bound sirolimus concentration is always higher than the unbound concentration, for the case of slow release polymer there is a inversion in this trend after the solid sirolimus depletion.

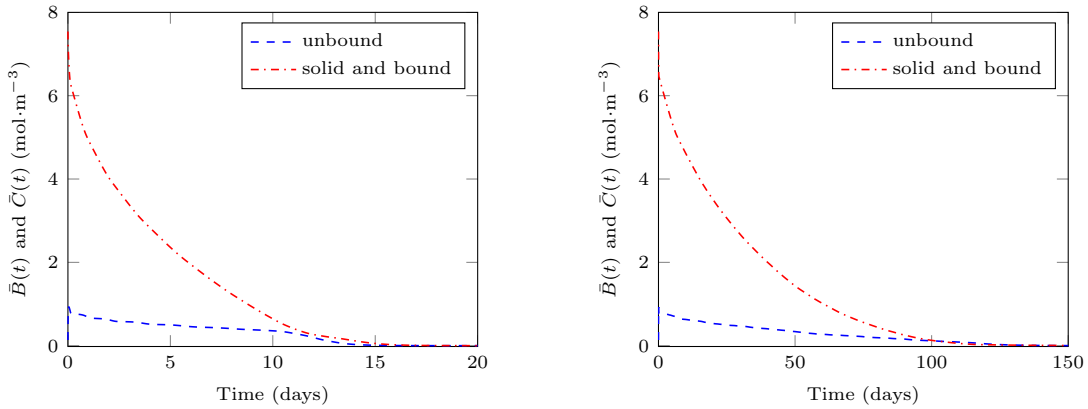

(a) (b)

Figure 13. (a) Time evolution of volume average sirolimus concentration of solid and bound ($b_0 + b_1 + b_2$ - red curve) and free ($c_0 + c_1$ - blue curve) for fast release polymer; (b) Time evolution of volume average sirolimus concentration of solid and bound ($b_0 + b_1 + b_2$ - red curve) and free ($c_0 + c_1$ - blue curve) for slow release polymer. The time scale is in days.

5. CONCLUSIONS

The simulation of the transport through a polymer layer and a porous arterial wall with binding in drug-eluting stent is performed. We consider the model of dissolution, transport and binding of sirolimus on an axisymmetric domain representing the polymer coating layer and the porous artery wall in the vicinity of a stent strut. We employ the FEM on an unstructured mesh to discretise the governing equations. On one hand, the nonlinear dissolution and diffusion in the polymer coating play a key role in determining the limiting time scale of the process. On the other hand, he nonlinear saturable binding model that includes both specific and non-specific binding in the arterial wall as separate phases plays an important role in determining the temporal-spatial distribution of the drug.

The effect of slow and fast release polymers is considered, showing that the time evolution of the process can be efficiently controlled by the polymer diffusion coefficient. The time evolution of the sirolimus average concentration is qualitatively similar for the cases of fast and slow release polymers, except by the fact that the time scale for the slow release polymer is much longer.

Using the sirolimus gradient at the interfaces, it is estimated that $46 - 48\%$ of the sirolimus is diffused to the lumen and it is lost to the flowing blood, while $52 - 54\%$ actually gets into the arterial wall. However, the spatial distribution of the sirolimus is greatly influenced by the flow and the arterial wall properties, being therefore susceptible to patient health conditions.

6. ACKNOWLEDGEMENTS

The authors would like to acknowledge financial support from FAPERJ, CNPq, and the University of Glasgow EPSRC GCF ISF fund.

7. REFERENCES

Bozsak, F., Chomaz, J. and Barakat, A., 2014. "Modelling the transport drugs of eluted from stents: physical phenomena driving drug distribution in the arterial wall". *Biomech Model Mechanobiol*, Vol. 13, pp. 327–347.

Chisari, A., Pistritto, A., Piccolo, R., Manna, A.L. and Danzi, G., 2016. "The ultimaster biodegradable-polymer sirolimus-eluting stent: An updated review of clinical evidence". *Int. J. Mol. Sci.*, Vol. 17(9), p. 1490.

Lucena, R.M., 2016. *Numerical study of CO2 dissolution in saline aquifers with deformed interface*. Ph.D. thesis, State University of Rio de Janeiro.

McGinty, S. and Pontrelli, G., 2016. "On the role of specific drug binding in modelling arterial eluting stents". *J Math Chem*, Vol. 54, pp. 967–976.

8. RESPONSIBILITY NOTICE

The authors are the only responsible for the printed material included in this paper.